Tetrahedron 66 (2010) 3360–3364

Contents lists available at ScienceDirect

Tetrahedron

journal homepage: www.elsevier.com/locate/tet

Crystal structures of *anti*- and *syn*-9,10-di(1′-naphthyl)anthracene and isomerization in solid state

Cho Hee Lee [a], Mi Jong Kim [a], Sang-Pil Han [a], Yoo-Soon Lee [a], Sung Kwon Kang [a], Jae Hee Song [b], Jong Tae Je [c], Hyoung-Yun Oh [d], Yeong-Joon Kim [a,*]

[a] Department of Chemistry, Chungnam National University, Daejeon 305-764, Republic of Korea
[b] Department of Chemistry, Sunchon National University, Sunchon 540-747, Republic of Korea
[c] SFC Co., Ltd, Ochang TechnoVillage 641-5, Gak-ri, Cheongwon, Chungbuk 363-883, Republic of Korea
[d] LG Display R&D Center, 1007 Deongeun-ri, Wollong-myeon, Paju-si Gyeonggi-do 413-811, Republic of Korea

ARTICLE INFO

Article history:
Received 13 November 2009
Received in revised form
21 February 2010
Accepted 22 February 2010
Available online 1 March 2010

Keywords:
Isomerization
Aryl–aryl rotation
X-ray structure
Anthracene

ABSTRACT

9,10-Di-(1′-naphthyl)anthracene is often used as electroluminescence materials in organic light-emitting diodes. Because of the hindered rotation about the σ-bond between naphthyl and anthracene chromophore, two possible stereoisomers can be isolated. HPLC, ^{1}H NMR, and ^{13}C NMR spectra gave two different sets of peaks and the X-ray single crystal analysis confirmed the structures of the two isomers, *anti* and *syn*. *syn* was more soluble than *anti* in THF as well as toluene and the thermal properties of the two were quite different. Differential scanning calorimetry study and HPLC analysis showed that the isomerization between *anti* and *syn* in the solid state took place at >370 °C.

1. Introduction

Conjugated aromatic compounds have attracted great interest from not only scientific but also industrial community because of their potential applications in the field of organic electronics such as organic thin film transistors (OTFTs) and organic light-emitting diodes (OLEDs). Anthracene derivatives have been the important ones among many of the leading materials due to their fluorescence characteristics from the anthracene chromophore and many studies have found applications as important class of highly efficient, stable, blue-light emitting materials as well as new class of host luminescent materials.[1–12] However, there is a significant electronic interaction between the chromophores in solid phase, which results in an undesired broadening of the emission spectrum and low fluorescence yield. To overcome this weakness, bulky substituents at 9 and 10 positions of anthracene are typically employed and the several compounds have been developed. 9,10-Di(1′-naphthyl)anthracene is a good example, where the rigid naphthyl substituents effectively isolate the anthracene chromophore, generating blue EL.

9,10-Diarylanthracenes, when the substituent groups are bulky, basically have two stereoisomers due to the hindered rotation about the σ-bond between aryl and anthracene moiety. Several calculations on these types of molecules have been reported and the barrier of rotation is known to be 35–40 kcal/mol. In fact, the rotational energy barrier for 1,9′-naphthylanthracene is calculated as 38.08 kcal/mol using B3LYP/6-31G*//HF/3-21G method.[13]

If the physical properties of the two stereoisomers are different, it is very important to study on the isolation and characterization of the isomers. In fact, Bard group published a paper many years ago dealing with the electrochemistry of 9,10-di(1′-naphthyl)anthracene and predicted the possibility of different electrical properties of the two isomers.[14] However, no such study has been done yet. Very recently, Linker et al. have published an elegant paper about the synthesis and characterization of stereoisomers of 9,10-diarylanthracenes with *ortho*-substituted phenyl.[15] We believe that 9,10-di(1′-naphthyl)anthracene is a more interesting molecule in industry because of the actual use of this molecule as OLED material in the current market. In terms of the process and working condition on OLED, the thermal stability and isomerization temperature of the two stereoisomers are also key factors to be considered. Here we report the crystalline structures from X-ray diffraction results of

* Corresponding author. Tel.: +82 42 821 5476; fax: +82 42 821 8896; e-mail address: y2kim@cnu.ac.kr.

0040-4020/$ – see front matter © 2010 Elsevier Ltd. All rights reserved.
doi:10.1016/j.tet.2010.02.072

the two isomers, *anti* and *syn* of 9,10-di(1′-naphthyl)anthracene (Fig. 1) and the solid state isomerization between the two at high temperature.

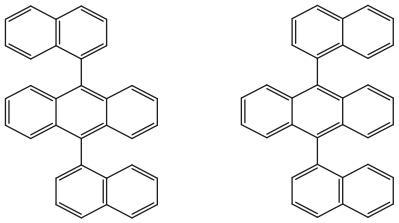

Figure 1. The structure of two stereoisomers of 9,10-di(1′-naphthyl)anthracene.

2. Results and discussion

The preparation of 9,10-di(1′-naphthyl)anthracene was followed the known procedures.[16–18] The product was obtained as yellow powder and the existence of two isomers was confirmed by HPLC, ^{1}H NMR, and ^{13}C NMR spectra.

The separation of two isomers was successfully performed after several times of recrystallization from toluene and xylene. To assign the structures of isomers, we performed X-ray analysis of the single crystals. Both *anti* and *syn* crystals were grown by slow evaporation of THF/hexane solution.

X-ray intensity data were collected on a Bruker SMART APEX-II CCD diffractometer using graphite monochromated Mo Kα radiation (λ=0.71073 Å). Structure was solved by applying the direct method using a SHELXS-97 and refined by a full-matrix least-squares calculation on F^2 using SHELXL-97.[19] All non-hydrogen atoms were refined anisotropically. All hydrogen atoms were placed in ideal positions and were riding on their respective carbon atoms (B_{iso}=1.2 B_{eq}). *anti* Isomer was refined with solvent free. Crystallographic data for the structure reported here have been deposited with the Cambridge Crystallographic Data Center (deposition nos. CCDC 722475 and CCDC 722476).

The Crystallographic data and refinement parameters for *anti*- and *syn*-isomers are summarized in Table 1. The selected bond distances and angles are summarized in Table 2. And an ORTEP view including the atomic numbering scheme is shown in Figure 2. In *anti* isomer, there is a crystallographic inversion center located in the center of anthracene ring. The dihedral angles between anthracene and naphthyl planes are 80.0(1)° and 82.2(2)° for *anti* and *syn*, respectively. As shown in Figure 3, *syn* isomer molecules are held together. The intermolecular distance of 3.670(4) Å between the two centroids of rings, symmetry code $-x$, y, $-z+1.5$, in the packing structure indicates that the crystal structure of *syn*-9,10-di(1′-naphythyl)anthracene is stabilized by π–π interaction between the two anthracene rings. And there is another weak intermolecular C–H···π interaction not shown in Figure 3 (the intermolecular distances between the C9–C14 ring and H33, H34 atoms are in the range of 2.841(3)–3.397(4) Å). X-ray single crystal structure of pyridine solvated *anti*-9,10-di(1′-naphthyl)anthracene has been reported and there seems to be stabilization by weak intermolecular C–H···N and C–H···π interactions.[20]

Table 1
Crystal data for two structures of 9,10-di(1′-naphthyl)anthracene

	anti	*syn*
Chemical formula	$C_{34}H_{22}$	$C_{34}H_{22}$
Formula weight	430.52	430.52
Temperature [K]	174(2)	295(2)
Wavelength [Å]	0.71073 Å	0.71073
Crystal system, space group	Monoclinic, *C*2/*c*	Monoclinic, *C*2/*c*
a [Å]	14.671(3)	18.1453(10)
b [Å]	10.131(2)	16.5882(10)
c [Å]	21.231(4)	14.8692(7)
β (°)	101.27(3)	96.094(3)
Volume [Å^3]	3094.8(11)	4450.3(4)
Z	4	8
F(000)	904	1808
Crystal size [mm]	0.20×0.18×0.16	0.11×0.06×0.06
Theta range for data collection	1.96–28.31°	1.67–25.49°
Reflections collected/unique	16,021/3849 [R_{int}=0.0385]	19,091/4127 [R_{int}=0.0816]
Data/restraints/parameters	3849/0/154	4127/0/328
Goodness-of-fit on F^2	1.052	0.937
Final *R* indices [$I>2\sigma(I)$]	R_1=0.0494, wR_2=0.1290	R_1=0.0653, wR_2=0.1521
R indices (all data)	R_1=0.0740, wR_2=0.1373	R_1=0.2016, wR_2=0.2175
Largest diff. peak and hole [e Å^{-3}]	0.214 and −0.223	0.189 and −0.194

Table 2
Selected bond distances (Å) and bond angles (°) of 9,10-di(1′-naphthyl)anthracene

	anti	*syn*
C1–C2	1.406(2)	1.414(5)
C1–C7^{i}	1.406(2)	
C1–C8	1.498(2)	
C1–C14		1.394(5)
C1–C15		1.498(5)
C2–C3	1.433(2)	1.411(5)
C2–C7	1.440(2)	1.450(5)
C3–C4	1.348(2)	1.361(5)
C4–C5	1.418(2)	1.413(5)
C5–C6	1.352(2)	1.336(6)
C6–C7	1.429(2)	1.440(5)
C2–C1–C7^{i}	120.0(1)	
C7^{i}–C1–C8	119.9(1)	
C2–C1–C8	120.1(1)	
C1–C2–C3	121.9(1)	122.2(4)
C3–C2–C7	117.9(1)	119.0(4)
C2–C1–C14		120.7(4)
C14–C1–C15		119.3(3)
C2–C1–C15		120.0(4)

Symmetry code: (i) x, $y+1$, z.

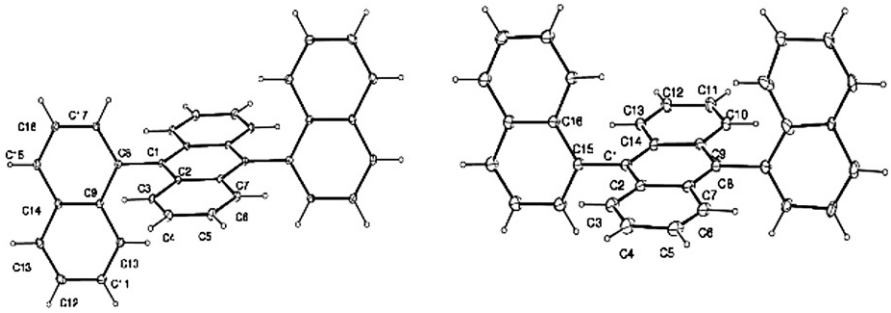

Figure 2. ORTEP drawings of two structures of the title compound with atom-numbering scheme; *anti* (left) and *syn* (right).

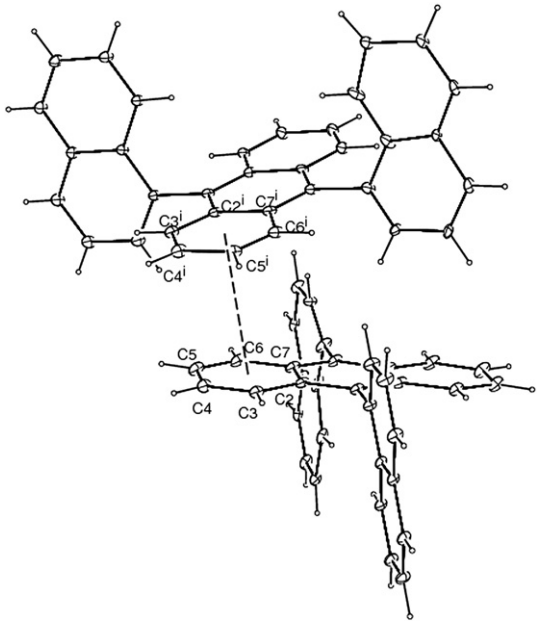

Figure 3. The π–π interaction (dashed line) between two rings in *syn* isomer (symmetry code; (i) $-x, y, -z+1.5$).

The assignment of the two HPLC peaks was possible after obtaining the X-ray diffraction data of the two isomers. The *syn* came first when the separations were performed on a 250 mm×4.6 mm column packed with 5 μm C_{18} bonded silica (Waters 600I, mobile phase was a mixture of H_2O/MeCN (5:95, v/v) with a flow rate of 1.5 ml/min.), which means the *syn* is more polar than *anti*. The following results for the ratio of *syn* to *anti* were from the HPLC analysis.

There were many procedures reported for the synthesis of 9,10-di(1′-naphthyl)anthracene. We followed three different literature conditions and compared the ratio of *syn* and *anti* isomers. The first synthetic method that we used was reduction of 9,10-di(1′-naphthyl)-9,10-dihydroanthracene-9.10-diol with KI/NaH_2PO in acetic acid.[16] The second method was the reaction of 9,10-dibromoanthracene with tri(1-naphthyl)indium in the presence of Pd catalyst.[17] The third method was the Suzuki–Miyaura reaction of 9,10-dibromoanthracene with 1-naphthaleneboronic acid.[18] All three reactions gave the product in good yields in the similar ratio of *anti*/*syn* as 50:50 (±5). A large deviation from the 50:50 *anti*/*syn* ratio was expected from the first method since the diol is known to be mainly in the *anti* configuration. This result tells that the steric effect is not a key issue in the reduction reaction of 9,10-di(1′-naphthyl)-9,10-dihydroanthracene-9.10-diol.

The product right after the synthesis shows ^{1}H NMR spectrum in Figure 4(c). After successful separation of two isomers, ^{1}H NMR spectrum of each isomer was much simpler as shown in Figure 4(a) and (b) and the spectrum of the mixture turns out simply the sum of

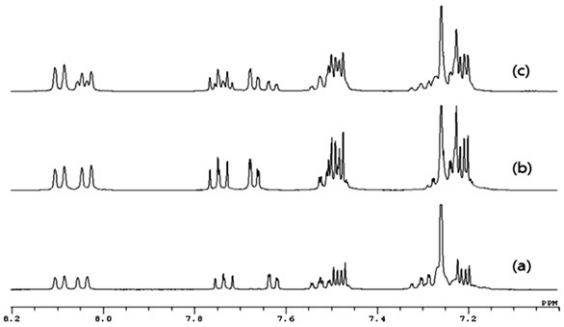

Figure 4. ^{1}H NMR spectra of 9,10-di(1′-naphthyl)anthracene in chloroform-*d* (a) *syn* (b) *anti* (c) mixture.

that of *syn* and *anti*. The ^{1}H NMR spectra of *syn* and *anti* in toluene-d_8 did not change until ca. 100 °C, which means the rotation of σ-bond between anthracene and naphthalene is very slow at that temperature and isomerization study could not be performed using solution NMR technique. The ^{13}C NMR spectrum of *anti* shows 14 peaks whereas that of *syn* has much more than 14 peaks with lower intensities. We interpret this phenomenon for *syn* as breaking symmetry due to the steric congestion. Figure 5 shows the UV and PL spectra of *anti* and *syn* in THF. There was no difference between *anti* and *syn* in solution state even though solid structures were different.

The solubility of the two isomers was quite different. Both *syn* and *anti* were more soluble in toluene than in THF. *syn* was more soluble than *anti* in THF as well as in toluene and the comparison of the values is shown in Table 3. This makes the large errors in obtaining the product ratio of *anti* to *syn* since the recrystallization makes higher ratio for *anti*.

We have tried to get melting points for the two isomers since the previous reports gave the only one for the mixture. *anti* crystal started to crumple at 369 °C and *syn* did not melt until 400 °C, which is the limit of the thermometer. The mixture started to melt

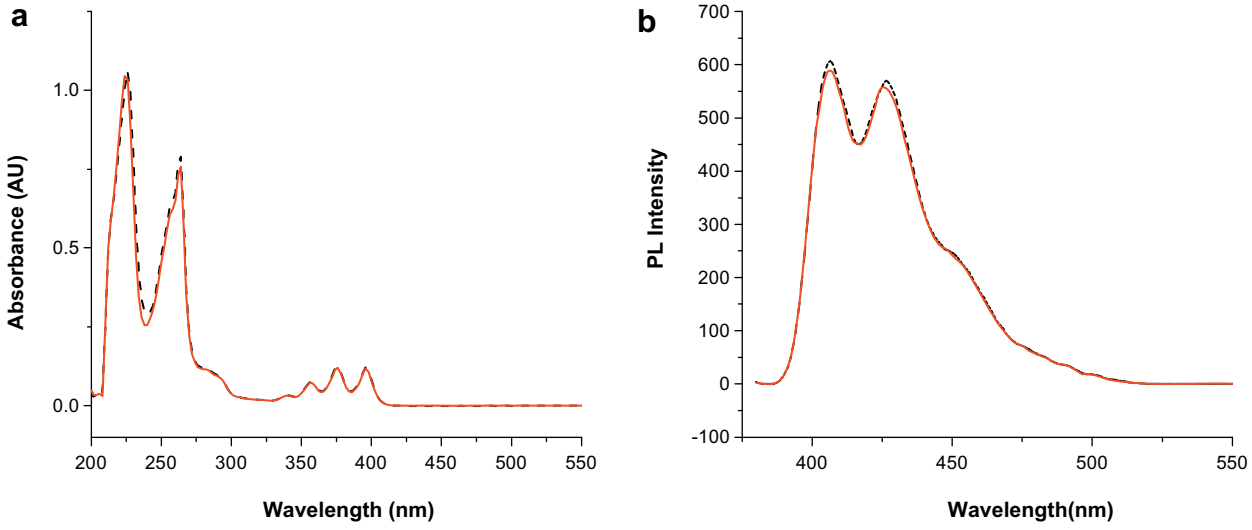

Figure 5. (a) Absorption (UV–vis) and (b) emission (PL) spectra of *anti* (—) and *syn* (…) in THF.

Table 3
Solubility of the *anti* and *syn* isomers in organic solvents

Solvent	*anti* (M)	*syn* (M)
THF	9.49×10^{-4}	1.04×10^{-3}
Toluene	1.99×10^{-3}	2.60×10^{-3}

from 360 °C as reported in the literature.[17] Since the thermal properties such as melting and sublimation temperature is very important in OLED, the extensive studies were conducted using DSC. *anti* has thermal profiles with three endothermic troughs, two shallow ones around 369 °C, and 376 °C, and a deep one around 409 °C as shown in Figure 6. The DSC profile for *syn* shows only one trough around 409 °C, which is very similar to the last one for that of *anti*. The large endotherm at 409 °C is due to melting for both isomers.

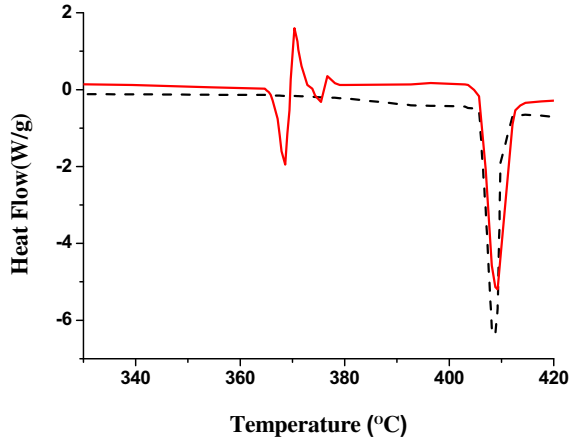

Figure 6. DSC curves of *anti* (—) and *syn* (…) on a heating scan at 10 deg min^{-1}.

To get an idea why *anti* has small DSC signals near 370 °C, HPLC analysis has been performed in connection with DSC experiment. The pure *anti* or *syn* solid was heated using DSC on a scan rate of 10 °C min^{-1} and the heating was stopped at every 10 °C interval from 340 °C to 440 °C. After cooling the samples, HPLC analysis gave the *anti*/*syn* ratio of each sample and the results were plotted in Figure 7.

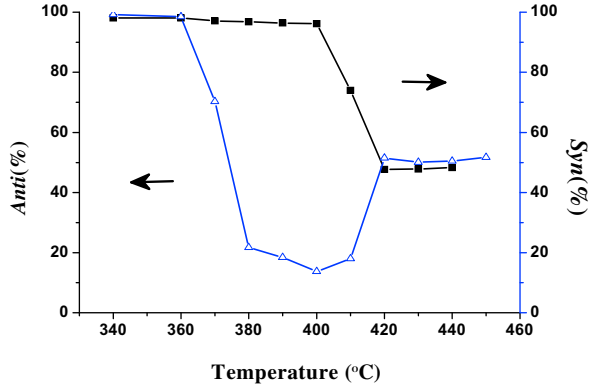

Figure 7. Mole percent changes of *syn* (■) and *anti* (△) at various temperatures.

Starting with 100% *anti,* the isomerization occurs at 370 °C and the percentage of *anti* dramatically dropped to 20% at 400 °C. After that the melting process reconstructs the new *anti*/*syn* equilibrium at 50:50. In contrast to this, starting with 100% *syn*, there was no isomerization until melt at 409 °C. Again, the *anti*/*syn* ratio reached to 50:50 after melting. This result means the stability of *anti* and *syn* is nearly equal, which is consistent with the calculation results in gas phase.[1]

The DSC in the connection with HPLC experiment clearly shows that the small DSC signals from 369 °C to 376 °C are due to the isomerization process from *anti* to *syn*. This is a feature of how the opposite isomer can fit into the crystal lattice.

The thermodynamic data for the DSC features of the *anti* at 368.5 °C and 376 °C show a near cancellation of endothermic and exothermic. Therefore there is no net heat. We would interpret that as an isomerization of ~30% of the *anti* at 369 °C, where the lattice softens enough to permit this. However, this produces *syn* in an unfavorable crystal environment, so the process is endothermic. Relaxation of the crystal at 371 °C is then exothermic, by an equal amount. Likewise at 375.5 °C another 40% of the *anti* isomerizes.

In summary, two isomers, *anti*- and *syn*-9,10-di-(1′-naphthyl)anthracene were isolated and characterized with X-ray, ^{1}H NMR, and ^{13}C NMR. This is unprecedented even though 9,10-di-(1′-naphthyl)anthracene is an important compound in organic electronics industry. DSC study and HPLC analysis provided the evidence of the isomerization between the *syn* and *anti* in solid state at high temperature. Since *syn* and *anti* have different physical properties in terms of solubility and thermal properties, the existence of stereoisomers should be an important factor to be considered in OLED.

3. Experimental

3.1. General information

All reagents and solvents including bromonaphthalene, anthraquinone were purchased from commercial sources and used as received. 9,10-Di(1′-naphthyl)anthracene was prepared by literature procedures.[16–18] The isolation of *anti* and *syn* isomers was successfully performed after several times of recrystallization from toluene and xylene. Both *anti* and *syn* single crystals were grown by slow evaporation of THF/hexane solution. ^{1}H and ^{13}C NMR spectra were recorded on a JEOL JNM-AL400 spectrometer, operating at 9.39 T. X-ray intensity data were collected on a Bruker SMART APEX-II CCD diffractometer using graphite monochromated Mo Kα radiation (λ=0.71073 Å). The ratio of *anti*/*syn* was monitored using LC–UV (Waters 600I). Separations were performed on a 250 mm×4.6 mm column packed with 5 μm C_{18} bonded silica. DSC was carried out on a TA instruments DSCQ10 differential scanning calorimeter with a 10 deg min^{-1} heating rate under nitrogen atmosphere. UV and PL spectra were obtained using an HP8452A and a PERKIN ELMER LIMITED LR64912C (λ_{ex}=376 nm), respectively.

3.1.1. anti-9,10-Di-(1′-naphthyl)anthracene. Mp 409 °C (from DSC); ^{1}H NMR (400 MHz, $CDCl_3$) δ 8.09 (d, J=8.4 Hz, 2H), 8.03 (d, J=8.0 Hz, 2H), 7.74 (dd, J=7.2, 8.0 Hz, 2H), 7.66 (d, J=6.8 Hz, 2H), 7.49 (m, 6H), 7.21(m, 8H); ^{13}C NMR (100 MHz, $CDCl_3$) δ 136.77, 135.38, 133.73, 133.65, 130.68, 129.29, 128.25, 128.16, 127.14, 126.76, 126.31, 126.03, 125.61, 125.24.

3.1.2. syn-9,10-Di-(1′-naphthyl)anthracene. Mp 409 °C (from DSC); ^{1}H NMR (400 MHz, $CDCl_3$) δ 8.09 (d, J=8.0 Hz, 2H), 8.04 (d, J=8.0 Hz, 2H), 7.73 (dd, J=7.2, 8.0 Hz, 2H), 7.62 (d, J=7.2 Hz, 2H), 7.50 (m, 6H), 7.30 (m, 4H), 7.21 (m, 4H); ^{13}C NMR (100 MHz, $CDCl_3$) δ 138.58, 136.77, 135.41, 133.82, 133.74, 133.62, 130.96, 130.74, 130.68, 129.24, 129.05, 128.92, 128.41, 128.29, 128.16, 127.56, 127.12, 126.69, 126.36, 126.06, 125.67, 125.63, 125.37, 125.26.

Acknowledgements

This work was supported by the Ministry of Knowledge Economy, Republic of Korea. C.H.L. is recipient of BK21 fellowship (2009).

References and notes

1. Raghunath, P.; Reddy, M. A.; Gouri, C.; Bhanuprakash, K.; Rao, V. J. *J. Phys. Chem.* **2006**, *A110*, 1152–1162.
2. Pope, M.; Kallmann, H. P.; Magnante, P. *J. Chem. Phys.* **1963**, *38*, 2042–2043.
3. Zhang, X. H.; Liu, M. W.; Wong, O. Y.; Lee, C. S.; Kwong, H. L.; Lee, S. T.; Wu, S. K. *Chem. Phys. Lett.* **2003**, *369*, 478–482.
4. Reddy, M. A.; Thomas, A.; Srinivas, K.; Rao, V. J.; Bhanuprakash, K.; Sridhar, B.; Kumar, A.; Kamalasanan, M. N.; Srivastava, R. *J. Mater. Chem.* **2009**, *19*, 6172–6184.
5. Cao, W. D.; Zhang, X. H.; Bard, A. J. *J. Electroanal. Chem.* **2004**, *566*, 409–413.
6. Yang, B.; Kim, S. K.; Xu, H.; Park, Y. I.; Zhang, H. Y.; Gu, C.; Shen, F. Z.; Wang, C. L.; Liu, D. D.; Liu, X. D.; Hanif, M.; Tang, S.; Li, W. J.; Li, F.; Shen, J. C.; Park, J. W.; Ma, Y. G. *ChemPhysChem* **2008**, *9*, 2601–2609.
7. Barraza-Jimenez, D.; Flores-Hidalgo, A.; Glossman-Mitnik, D. *J. Mol. Struct. (Theochem)* **2009**, *894*, 64–70.
8. Tao, S.; Peng, Z.; Zhang, X.; Wu, S. *J. Lumin.* **2006**, *121*, 568–572.
9. Bard, A. J. *Electrogenerated Chemiluminescence*; Marcel Dekker: New York, NY, 2004; pp. 523–532.
10. Danel, K.; Huang, T. H.; Lin, J. T.; Tao, Y. T.; Chuen, C. H. *Chem. Mater.* **2002**, *14*, 3860–3865.
11. Kim, S. K.; Yang, B.; Park, Y. I.; Ma, Y. G.; Lee, J. Y.; Kim, H. J.; Park, J. *Org. Electron.* **2009**, *10*, 822–833.
12. Kwon, S.-K.; Kim, Y.-H.; Park, S.-Y.; An, B.-K. *Mol. Cryst. Liq. Cryst.* **2002**, *377*, 19–23.
13. Nori-shargh, D.; Asadzadeh, S.; Ghanizadeh, F. R.; Deyhimi, F.; Amini, M. M.; Jameh-Bozorghi, S. *J. Mol. Struct. (Theochem)* **2005**, *717*, 41–51.
14. Marcoux, L. S.; Lomax, A.; Bard, A. J. *J. Am. Chem. Soc.* **2002**, *92*, 243–250.
15. Zehm, D.; Fudickar, W.; Hans, M.; Schilde, U.; Kelling, A.; Linker, T. *Chem.—Eur. J.* **2008**, *14*, 11429–11441.
16. Smet, M.; Van Dijk, J.; Dehaen, W. *Tetrahedron* **1999**, *55*, 7859–7874.
17. Lee, W.; Kang, Y.; Lee, P. H. *J. Org. Chem.* **2008**, *73*, 4326–4329.
18. Hassan, J.; Sevignon, M.; Gozzi, C.; Schulz, E.; Lemaire, M. *Chem. Rev.* **2002**, *102*, 1359–1469.
19. Sheldrick, G. *Acta Crystallogr.* **2008**, *A64*, 112–122.
20. Lee, C. H.; Kim, M. J.; Kim, Y.-J.; Je, J. T.; Lee, Y.-S.; Kang, S. K. *Acta Crystallogr.* **2009**, *E65*, o2842.